Evolution of the Electronic Structure of 1T-Cu_xTiSe_2

J. F. Zhao,[1] H. W. Ou,[1] G. Wu,[2] B. P. Xie,[1] Y. Zhang,[1] D. W. Shen,[1] J. Wei,[1] L. X. Yang,[1] J. K. Dong,[1] M. Arita,[3] H. Namatame,[3] M. Taniguchi,[3] X. H. Chen,[2] and D. L. Feng[1,*]

[1]*Department of Physics, Applied Surface Physics State Key Laboratory, and Advanced Materials Laboratory, Fudan University, Shanghai 200433, People's Republic of China*

[2]*Hefei National Laboratory for Physical Sciences at Microscale and Department of Physics, University of Science and Technology of China, Hefei, Anhui 230026, People's Republic of China*

[3]*Hiroshima Synchrotron Radiation Center and Graduate School of Science, Hiroshima University, Hiroshima 739-8526, Japan*

(Received 19 January 2007; published 1 October 2007)

The electronic structure of a new charge-density-wave system or superconductor, 1T-Cu_xTiSe_2, has been studied by photoemission spectroscopy. A correlated semiconductor band structure is revealed for the undoped case, which resolves a long-standing controversy in the system. With Cu doping, the charge-density wave is suppressed by the raising of the chemical potential, while the superconductivity is enhanced by the enhancement of the density of states, and possibly suppressed at higher doping by the strong scattering.

DOI: 10.1103/PhysRevLett.99.146401 PACS numbers: 71.20.−b, 71.45.Lr, 79.60.−i

Transition metal dichalcogenides (TMD's) provide an important playground of interesting physics, such as charge density wave (CDW) and superconductivity [1]. Different chemical and structural configurations cause dramatic changes of their properties. In the CDW state, an energy gap opens at the Fermi surface of 1T-structured TaS_2 [2], but only partially opens for the 2H-structured TaS_2 [3], whereas there is no gap for 1T-$TiSe_2$ [4]. Moreover, superconductivity usually coexists and competes with CDW in 2H-structured TMD's [5–7], whereas it rarely exists in 1T structured compounds.

Recently, the discovery of superconductivity in 1T-Cu_xTiSe_2 has further enriched the physics of TMD's [8]. The undoped 1T-$TiSe_2$ is a CDW material, whose mechanism remains controversial after decades of research. For example, some considered the CDW a band-type Jahn-Teller effect, where the electronic energy is lowered through structural distortion [9,10]. Some considered it a realization of the excitonic CDW mechanism proposed by Kohn in the 1960's [11,12], but different models were proposed to interpret the electronic structure, depending on whether the system was argued to be a semimetal, or a semiconductor [13–15]. With Cu doping, it was found that the CDW transition temperature quickly drops, similar to other M_xTiSe_2's (M = Fe, Mn, Ta, V, Nb) [16–19]. Meanwhile, the superconducting phase emerges from $x \sim 0.04$ and reaches the maximal transition temperature (T_c) of 4.3 K at $x \sim 0.08$, then decreases to 2.8 K at $x \sim 0.10$. This phase diagram remarkably resembles those of the cuprate and heavy fermion superconductors [20], except here the competing order of superconductivity is the charge order, instead of the antiferromagnetic spin order. This ubiquitous phase diagram in 1T-Cu_xTiSe_2 calls for a detailed study of its electronic structure.

We studied 1T-Cu_xTiSe_2 with angle resolved photoemission spectroscopy (ARPES). A correlated semiconductor band structure of the undoped system is evidently illustrated, resolving a long-standing controversy. Cu doping is found to effectively enhance the density of states around the Fermi energy (E_F), which explains the enhancement of superconductivity. On the other hand, severe inelastic scattering was observed near the solubility limit, corresponding to the drop of superconducting transition temperature in that regime. With increased doping, chemical potential is raised, and signs of the weakening electron-hole coupling is discovered, which is responsible for the suppression of the CDW. Our results indicate that the seeming ''competition'' between CDW and superconductivity in the phase diagram is a coincidence caused by different effects of doping in this 1T compound, in contrast to the 2H-TMD case [3].

1T-Cu_xTiSe_2 single crystals were prepared by the vapor-transport technique, with doping $x = 0$, 0.015, 0.025, 0.055, 0.065 and 0.11 [21]. T_c's, for $x = 0.055$ and 0.065 are 2.5 and 3.4 K, respectively, similar to previous report [8]. Superconductivity is not observed down to 2 K for $x = 0.11$. Judging from the phase diagram, the CDW phase transition temperature T_{CDW}'s are about 220, 190, 170, and 70 K for $x = 0$, 0.015, 0.025 and 0.055, respectively, and doping 0.065 is just merely outside the CDW regime. ARPES experiments were performed with a Helium lamp or synchrotron radiation at beam line 9 of HiSOR. An angular resolution of 0.3° and an energy resolution of 10 meV were achieved with the Scienta R4000 electron analyzer. The samples were cleaved or measured in ultra-high vacuum ($\sim 5 \times 10^{-11}$ mbar).

Survey of the electronic structure was conducted with 21.2 eV He-Iα photons. The photoemission intensity distributions near E_F are projected onto the Γ-**K**-**M** or **A**-**H**-**L** plane for $x = 0$, 0.025, 0.055, and 0.065 in Figs. 1(a)–1(d), respectively. The perpendicular momentum of $k_{\|} = a^*/2$ electrons is close to that of **L** (thus denoted by **L**′), where a^* being the reciprocal lattice vector shown in Fig. 1(b) [14,22]. Strong spectral weight located

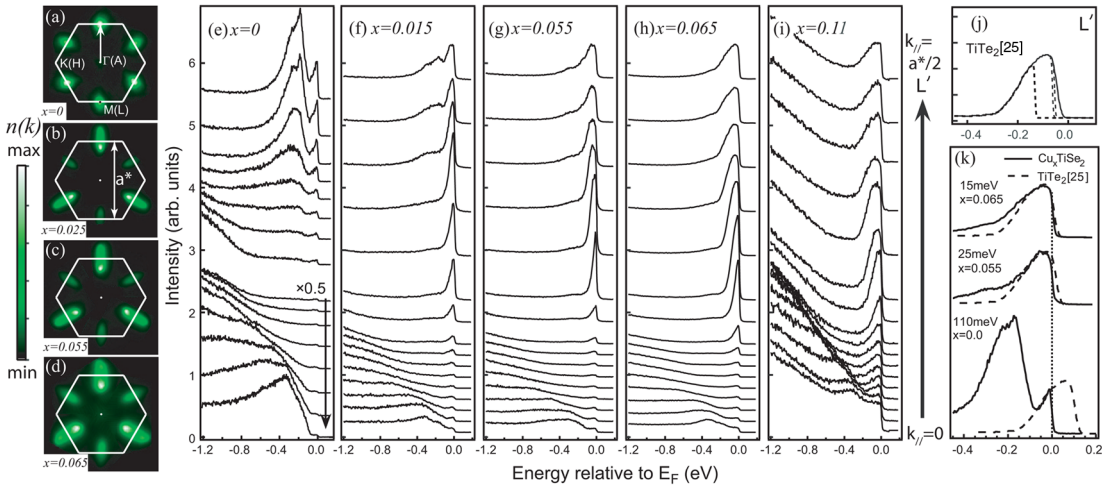

FIG. 1 (color online). (a)–(d) False color plot of the distribution of spectral weight integrated over ±40 meV around E_F for $1T$-Cu_xTiSe_2 with $x = 0$, 0.025, 0.055, and 0.065, respectively. Data were threefold symmetrized. (e)–(i) Photoemission spectra sampled equally along the $k_{\|} = 0 \rightarrow a^*/2$ cut shown in panel **a** for various Cu dopings. The spectra were stacked for clarity. (j) Photoemission spectrum of $TiTe_2$ at $\mathbf{L}'$ taken at 20 K with 21.2 eV photon from Ref. [25], where the three dashed curves are the simulated spectra when the chemical potential is shifted down by 15, 25, and 110 meV, respectively, (lifetime variation with doping is neglected). (k) Comparison of the shifted $TiTe_2$ spectra with the $\mathbf{L}'$ spectra for three dopings. All data were taken at $T = 20$ K.

around $\mathbf{L}'$ forms the so called Fermi patches [3], which expands with increased Cu doping, consistent with the previous susceptibility and ARPES data [8,23]. Symmetry of the trigonal lattice is manifested in the alternating strong and weak $\mathbf{L}'$ regions. As they show similar behaviors, we will focus on the data around the strong region hereafter.

Photoemission spectra taken at low temperatures along the cut sketched in Fig. 1(a) exhibit remarkable doping dependence [Figs. 1(e)–1(i)]. The flat-band feature at E_F around $\mathbf{L}'$ corresponds to the narrow Ti $3d$ band, which dominates the density of states near E_F. The highly dispersive features near $k_{\|} = 0$ are spin-orbit-split Se $4p$ bands [13,14], which are folded to the $\mathbf{L}$ region [Figs. 1(e)–1(g)] by the CDW. The Ti $3d$ band clearly extends from around the $\mathbf{L}'$ region towards $k_{\|} = 0$ with increased doping, causing significant increase of the density of states around E_F. Recent thermal conductivity data from $1T$-$Cu_{0.06}TiSe_2$ indicate that it is a single band s-wave superconductor [24]. Therefore, if the superconductivity here is of BCS kind as in the $2H$-TMD compounds [5,7], increased Cu doping would enhance it. However, when the Ti $3d$ band eventually reaches $k_{\|} = 0$ at $x = 0.11$ [Fig. 1(i)], the spectral background at high binding energies is severely enhanced, which has been confirmed in different batches of samples. Moreover, the residual resistivity ratio of the $x = 0.11$ sample is similar to the others [21]. Therefore, it suggests that high Cu concentrations would induce disorder effects such as enhanced inelastic scattering, which might be responsible for the suppression of superconductivity in this regime [8]. On the other hand, backward scattering that would enhance the residual resistivity seems not to be affected to the same extent.

The spectral linewidth of the Ti $3d$ band shows an intriguing increase with doping at the same momentum, while the midpoint of the spectral leading edge is about $3 \sim 4$ meV above E_F. In a conventional band structure sense, this would indicate the ''quasiparticle'' band has not crossed E_F up to the highest Cu doping. The observed sharp feature at low doping is just a Fermi-Dirac cutoff of a broad feature above E_F. Therefore, it grows broader with increasing doping, and eventually the peaks become rounded or even flat [Figs. 1(h) and 1(i)]. This remarkably resembles the line shape of $TiTe_2$ spectrum taken under the same condition [25], as reproduced in Fig. 1(j). $TiTe_2$ is a metal, whose Ti-$3d$-band feature at $\mathbf{L}'$ is just below E_F. In fact, if one would shift the chemical potential down by 15, 25, and 110 meV (with an uncertainty of about ±10 meV) [Fig. 1(j)], or equivalently shift the $TiTe_2$ spectra up [Fig. 1(k)], the $1T$-Cu_xTiSe_2 ($x = 0.065$, 0.055 and 0, respectively) spectra would be fitted surprisingly well. The differences at higher energies between the shifted spectra and the data are attributed to the folded Se $4p$ bands due to the CDW. $TiTe_2$ was considered to be a prototypical Fermi liquid system before. However, with much improved resolution, the many-body nature of $TiTe_2$ and $1T$-Cu_xTiSe_2 is exposed. In particular, our fitting shows that the sharp Ti $3d$ feature at $\mathbf{L}'$ for $x = 0$ is just a partially occupied spectral function, whose center-of-mass is actually *above* the Fermi energy, whereas most of the spectrum is recovered for $x = 0.065$, since it differs very little from the $1T$-$Cu_{0.11}TiSe_2$ or $TiTe_2$ spectrum.

The anomalous evolution of the Ti $3d$ state line shape requires reexamination of the band structure. Photoemission intensity along the Γ-$\mathbf{M}$, and $\mathbf{L}$-$\mathbf{A}$ directions were measured with 12.85 and 18.5 eV photons, respectively [13] (Fig. 2). Data at both low and high temperatures were compared. For $1T$-$TiSe_2$, the top of the valence band is located slightly below the Fermi energy at 250 K [Fig. 2(a)],

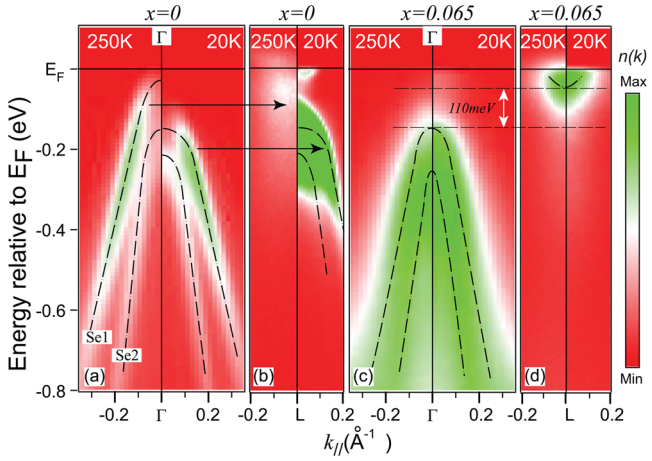

FIG. 2 (color online). Photoemission intensity map for (a)–(b) $1T$-$TiSe_2$ and (c)–(d) $1T$-$Cu_{0.065}TiSe_2$ at 20 and 250 K were compared near Γ and **L**. The dash-dotted line is the dispersion obtained from the MDC analysis. Arrows illustrate the band folding. Se1 and Se2 labels are assigned to the two Se $4p$ bands.

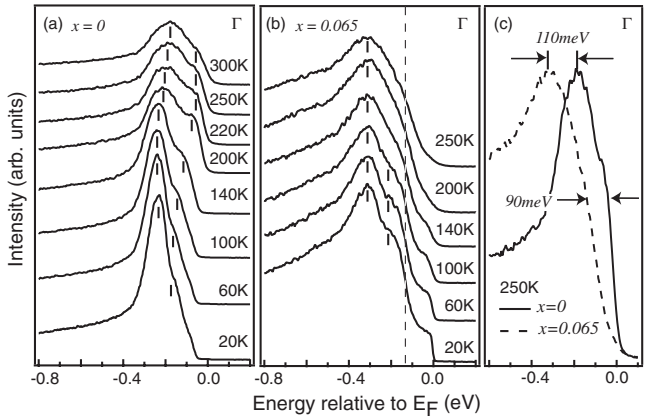

FIG. 3. Temperature dependence of the spectrum at Γ for (a) $1T$-$TiSe_2$, and (b) $1T$-$Cu_{0.065}TiSe_2$. (c) compares the spectral leading edges at Γ for these two dopings at 250 K.

while the Ti $3d$ band feature is quite weak and broad around E_F [Fig. 2(b)]. At 20 K, a large gap opens near Γ region, and the Se $4p$ bands are strongly folded to **L** region due to the formation of $2 \times 2 \times 2$ CDW [13]. The CDW fluctuations are strong even in the normal state, which induces band folding and possible small gap at Γ. Since thermal broadening above the CDW transition temperature further adds to the complication, whether the Se1 band and the Ti band overlap or not could not be definitely resolved, resulting in a controversial situation [13,14]. Fortunately, $1T$-$Cu_{0.065}TiSe_2$ provides an excellent opportunity to resolve this controversy. As shown in Figs. 2(c) and 2(d), the band position hardly moves at all with temperature in this compound as it is already out of the CDW phase. CDW fluctuations still exist, but only causes quite weak band folding. Therefore, the original band structure without much complication from the CDW and thermal broadening effects is revealed. Furthermore, as chemical potential shifts up with electron doping, the Ti $3d$ feature at **L** is almost fully recovered [Fig. 2(d)]. There is a clear gap as large as 110 meV between the Se1 and Ti $3d$ bands, whose position is defined by the centroid of the spectra. The undoped system is thus *undoubtedly* a semiconductor under this conventional definition. On the other hand, the broad "tails" of those two bands could overlap in-between the two dashed lines in Figs. 2(c) and 2(d). Subsequently, there are hole states near Γ, and electron states near **L** in the undoped system, making the system a weak semimetal in the many-body sense. This explains the plasma edge observed in the recent optical data of $TiSe_2$ [15].

Finer temperature evolution of the spectrum at Γ is shown in Fig. 3. For $1T$-$TiSe_2$, a large gap opens at the Se $4p$ bands when the system enters deeply into the CDW states [Figs. 3(a)], which causes a shift of about 110 meV and 50 meV for the Se1 and Se2 band, respectively. This helps lowering the energy of the CDW state. For $x =$ 0.065, such a shift is absent [Fig. 3(b)], the steplike feature at E_F comes from the extension of the Ti $3d$ bands plus possibly some weak folding [Fig. 2(c)]. Because the $1T$-$TiSe_2$ spectrum varies very little at high temperatures, one can estimate a chemical potential shift of about 100 ± 10 meV with 6.5% Cu doping both from the leading edge and the peak position [Fig. 3(c)]. The almost identical shifts of Se $4p$ and Ti $3d$ bands [Fig. 1(k)] illustrate the rigid band nature of the doping.

The folded Se $4p$ bands at **L** are found to weaken significantly with increased doping or temperature (Fig. 4), in correlation with the CDW strength, which was explained as the loss of long range CDW correlation earlier [23]. CDW fluctuations are quite robust in the

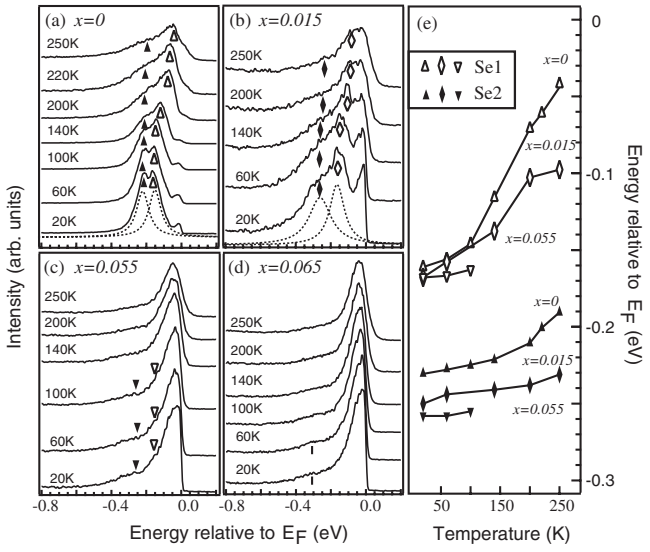

FIG. 4. Temperature dependence of the spectrum at **L** for (a) $x = 0$, (b) $x = 0.015$, (c) $x = 0.055$ and (d) $x = 0.065$. The spectra were stacked for clarity. The dashed lines are fit to help resolve the folded two Se $4p$ bands. (e) summarizes the temperature dependence of Se1 and Se2 positions in panels (a)–(d). Error bars of ±5 meV is neglected for a clearer view.

normal state. For $x = 0$, the spectrum at 250 K still contains significant contribution from the folding [Fig. 4(a)]. Similarly, in Figs. 4(b)–4(d), there also exists a small amount of residual folded weight well above T_{CDW}. Moreover, with increased temperature, the folded features shift toward E_F. For example, a shift of more than 110 meV for the folded Se1 band is observed in Fig. 4(a) for $TiSe_2$. The positions of the folded Se1 and Se2 bands are summarized in Fig. 4(e). One finds that the shift of the Se1 band is much larger than that of Se2 band in the studied temperature range. With increased doping, the maximal shift of the Se1 band drops faster than that of the Se2, and eventually they both diminish with the CDW. The correlation between the shift and CDW cannot be understood within the band Jahn-Teller picture, since the Jahn-Teller distortion would have gained more electronic energy through the filled Ti $3d$ band. On the other hand, if the shift of the Se bands are caused by the coupling between the electrons in the Se bands and holes in the Ti band (i.e., the excitonic effects), the decreasing shift of the Se bands with doping can be naturally explained by the weakening electron-hole interaction due to the raise of chemical potential. As the energy of the CDW state lowers through these shifts, the CDW strength would decrease with the weakening electron-hole interaction. Consistently, the indirect Jahn-Teller scenario proposed for the undoped system before [13], which includes electron-hole interactions and multiband effects, is also able to explain the above doping behavior. In this scenario, the degenerate conduction bands split and push down the valence band in the CDW state and thus gain energy [13]. Since Se1 band is closer to the conduction band, the hybridization will push it harder than the Se2 band [Fig. 4(e)].

Alternatively, the drop of CDW can be understood in the general excitonic picture proposed by Kohn [11], where an indirect-gap semiconductor is unstable against the formation of excitons between valence electrons and holes in the conduction band, if the exciton binding energy is higher than the energy difference between the electron and hole (i.e., band gap for a semiconductor). For $1T$-Cu_xTiSe_2, the measured chemical potential shift of 100 ± 10 meV for $x = 0.065$ makes the centroid of the valence band sufficiently below E_F and the exciton or CDW formation costly enough. Therefore, the CDW is suppressed at high doping. Compared with the exciton energy of 17 meV estimated [4], this large shift is necessary because the large linewidth would reduce the distance between the highest valence state and E_F significantly.

The CDW in $1T$-Cu_xTiSe_2 does not cause an energy gap for the Ti $3d$ band, which makes the large density of states at E_F almost unaffected. Therefore, there is plenty of spectral weight available for superconductivity. We found no direct evidence in the electronic structure that the CDW microscopically competes with superconductivity as might be expected from the phase diagram [8,23].

To summarize, $1T$-Cu_xTiSe_2 is proved to be a correlated semiconductor at zero doping, resolving a long-standing controversy, and the doping behavior of the CDW in this material can be well understood if electron-hole coupling is taken into account. The seeming competition between CDW and superconductivity in this system is very likely a coincidence, as Cu doping enhances the density of states and thus favors the superconductivity, while it also raises the chemical potential and thus weakens the charge-density wave simultaneously.

We gratefully acknowledge the helpful discussion with Professors Z. Y. Weng and D. H. Lee. This work was supported by NSFC, MOST (973 Project No. 2006CB601002 and No. 2006CB921300), and STCSM of China.

*dlfeng@fudan.edu.cn

[1] J. A. Wilson, F. J. Di Salvo, and S. Mahajan, Adv. Phys. **24**, 117 (1975).
[2] Th. Pillo *et al.*, Phys. Rev. Lett. **83**, 3494 (1999).
[3] D. W. Shen *et al.*, arXiv:cond-mat/0612064.
[4] P. Aebi *et al.*, Phys. Rev. B **61**, 16 213 (2000), and reference therein.
[5] T. Valla *et al.*, Phys. Rev. Lett. **92**, 086401 (2004).
[6] A. H. Castro Neto, Phys. Rev. Lett. **86**, 4382 (2001).
[7] T. Yokoya *et al.*, Science **294**, 2518 (2001).
[8] E. Morosan *et al.*, Nature Phys. **2**, 544 (2006).
[9] H. P. Hughes, J. Phys. C **10**, L319 (1977).
[10] K. Rossnagel, L. Kipp, and M. Skibowski, Phys. Rev. B **65**, 235101 (2002).
[11] W. Kohn, Phys. Rev. Lett. **19**, 439 (1967).
[12] J. A. Wilson and A. D. Yoffe, Adv. Phys. **18**, 193 (1969).
[13] T. E. Kidd, T. Miller, M. Y. Chou, and T.-C. Chiang, Phys. Rev. Lett. **88**, 226402 (2002), and references therein.
[14] P. Aebi, Th. Pillo, H. Berger, and F. Lévy, J. Electron Spectrosc. Relat. Phenom. **117–118**, 433 (2001).
[15] G. Li *et al.*, Phys. Rev. Lett. **99**, 027404 (2007).
[16] X. Y. Cui *et al.*, Phys. Rev. B **73**, 085111 (2006).
[17] F. J. Di Salvo and J. V. Waszczak, Phys. Rev. B **17**, 3801 (1978).
[18] F. Levy, J. Phys. C **13**, 2901 (1980).
[19] N. V. Baranov *et al.*, J. Phys. Condens. Matter **19**, 016005 (2007).
[20] E. Dagotto, Science **309**, 257 (2005).
[21] For detailed sample description, see G. Wu *et al.*, Phys. Rev. B **76**, 024513 (2007).
[22] With Cu intercalation, c only increases by 1% at the maximum concentration. Our synchrotron experiments show that the photon energy corresponding to particular momentum varies negligibly with dopings.
[23] D. Qian *et al.*, Phys. Rev. Lett. **98**, 117007 (2007).
[24] S. Y. Li, L. Taillefer, G. Wu, and X. H. Chen, Phys. Rev. Lett. **99**, 107001 (2007).
[25] R. Claessen *et al.*, Phys. Rev. B **54**, 2453 (1996).